AD-A035 473 ROME AIR DEVELOPMENT CENTER GRIFFISS AFB N Y F/G 20/5
EXTINCTION OF DF LASER RADIATION DERIVED FROM OUTDOOR ATMOSPHER--ETC(U)
DEC 76 J W CUSACK
UNCLASSIFIED RADC-TR-76-333 NL

1 OF 1
ADA035473

END

DATE
FILMED
3 - 77

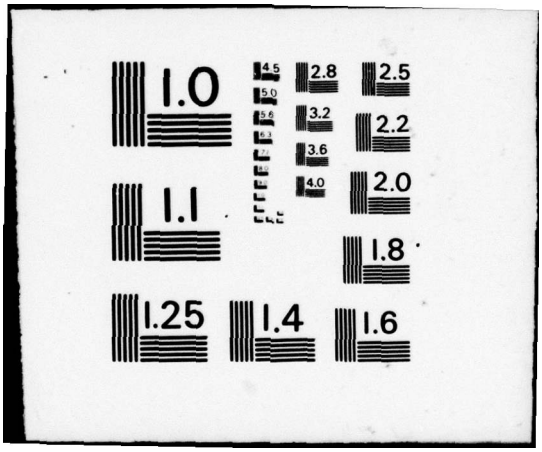
1.0
1.1
1.25
1.4
1.6
1.8
2.0
2.2
2.5
2.8
3.2
3.6
4.0
4.5
5.0

RADC-TR-76-333
In-House Technical Report
December 1976

EXTINCTION OF DF LASER RADIATION DERIVED FROM OUTDOOR ATMOSPHERIC MEASUREMENTS

James W. Cusack

Sponsored By
Defense Advanced Research Projects Agency (DoD)
ARPA Order No. 1279

ROME AIR DEVELOPMENT CENTER
AIR FORCE SYSTEMS COMMAND
GRIFFISS AIR FORCE BASE, NEW YORK 13441

This report has been reviewed by the RADC Information Office (OI) and is releasable to the National Technical Information Service (NTIS). At NTIS it will be releasable to the general public including foreign nations.

This report has been reviewed and is approved for publication.

APPROVED: Vincent J. Coyne

VINCENT J. COYNE
Chief, Space Surveillance &
Instrumentation Branch

APPROVED: Joseph L. Ryerson

JOSEPH L. RYERSON
Technical Director
Surveillance Division

FOR THE COMMANDER: John P. Huss

JOHN P. HUSS
Acting Chief, Plans Office

Do not return this copy. Retain or destroy.

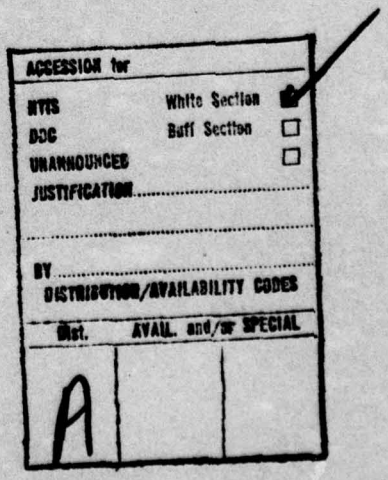

EXTINCTION OF DF LASER RADIATION DERIVED FROM OUTDOOR ATMOSPHERIC MEASUREMENTS

James W. Cusack

Contractor: N/A
Contract Number: N/A
Effective Date of Contract: N/A
Contract Expiration Date: N/A
Short Title of Work: N/A
Program Code Number: 4E20
Period of Work Covered: Jul 74 - Jul 76

Principal Investigator: N/A
Project Engineer: James W. Cusack
Phone: 315 330-3145

This research was supported by the Defense Advanced Research Projects Agency of the Department of Defense and was monitored by James W. Cusack (OCSE), Griffiss AFB NY 13441.

UNCLASSIFIED

SECURITY CLASSIFICATION OF THIS PAGE (When Data Entered)

REPORT DOCUMENTATION PAGE

READ INSTRUCTIONS BEFORE COMPLETING FORM

1 REPORT NUMBER: RADC-TR-76-333	2 GOVT ACCESSION NO.
3 RECIPIENT'S CATALOG NUMBER: (9)	
4 TITLE (and Subtitle): EXTINCTION OF DF LASER RADIATION DERIVED FROM OUTDOOR ATMOSPHERIC MEASUREMENTS. (6)	5 TYPE OF REPORT & PERIOD COVERED: In-House Technical Report.
	6 PERFORMING ORG. REPORT NUMBER: N/A
7 AUTHOR(s): (10) James W. Cusack	8 CONTRACT OR GRANT NUMBER(s): N/A (12) 35p.
9 PERFORMING ORGANIZATION NAME AND ADDRESS: Rome Air Development Center (OCSE) Griffiss AFB NY 13441	10 PROGRAM ELEMENT, PROJECT, TASK AREA & WORK UNIT NUMBERS: 62301E 12790501
11 CONTROLLING OFFICE NAME AND ADDRESS: Defense Advanced Research Projects Agency 1400 Wilson Blvd Arlington VA 22209 (11)	12 REPORT DATE: December 1976
	13 NUMBER OF PAGES: 26
14 MONITORING AGENCY NAME & ADDRESS(if different from Controlling Office): Rome Air Development Center (OCSE) Griffiss AFB NY 13441	15 SECURITY CLASS. (of this report): UNCLASSIFIED
	15a DECLASSIFICATION/DOWNGRADING SCHEDULE: N/A

16 DISTRIBUTION STATEMENT (of this Report)

Approved for public release; distribution unlimited.

(16) 1279 (17) 05

17 DISTRIBUTION STATEMENT (of the abstract entered in Block 20, if different from Report)

Same

18 SUPPLEMENTARY NOTES

RADC Project Engineer:
James W. Cusack (OCSE)

19 KEY WORDS (Continue on reverse side if necessary and identify by block number)

Lasers
Atmospheric optics
Propagation

20 ABSTRACT (Continue on reverse side if necessary and identify by block number)

Recent advancements in the development of the DF (Deuterium Flouride) laser as a high power device have prompted interest in better defining atmospheric propagation constants for the region of the infrared spectrum in which it emits, 3.5 to 4.0 microns. Existing low resolution spectroscopic studies of these wavelengths indicate that it is a "window" region and has reasonably better transmission characteristics than most of the infrared. This report covers outdoor field measurements of the atmospheric transmission of four dominant DF laser lines. The measurements were performed at the Advanced Optical

DD FORM 1 JAN 73 1473 EDITION OF 1 NOV 65 IS OBSOLETE

UNCLASSIFIED

SECURITY CLASSIFICATION OF THIS PAGE (When Data Entered)

309050

Test Facility located at the Verona Test Annex of the Rome Air Development Center. The measurements were made with a pulsed DF laser which was used to transmit across a propagation path of 2000 feet in length. Results are reported here for the 2-1 P(8), 2-1 P(9), 3-2 P(8) and the 2-1 P(6) DF lines. The experimental results are analyzed and compared with the latest in-laboratory measurements. Results indicate that in high humidity environments the differences between laboratory and field measurements become increasingly larger.

TABLE OF CONTENTS

LIST OF ILLUSTRATIONS

LIST OF TABLES

1.0 Introduction

A large portion of the infrared spectrum from 1 to 15 microns is severely attenuated by atmospheric constituents. However, within this spectral range there are "window" regions where transmission is relatively improved. One such region occurs between 3.5 and 4 microns and lies in the same region as the output of the DF laser. Since the DF laser is capable of high power output it has become a candidate for the various systems applications which require long path transmission through the atmosphere. At the present time some of the necessary atmospheric constants for this laser, specifically, atmospheric extinction, are still uncertain and a more accurate assessment of its transmission capabilities is required.

There are several important propagation effects which seriously limit the transmission of high energy laser radiation through the atmosphere. Of these, scattering, absorption, turbulence and thermal blooming play the dominant roles. The initial assessments of the molecular absorption of DF lasers were made on the basis of low resolution solar spectra. However, low resolution spectroscopy does not adequately describe the true extinction of high resolution monochromatic laser radiation since at this fine resolution, atmospheric absorption becomes highly frequency dependent. Because of this inadequacy alternative techniques are being pursued and, where direct measurements are required, a DF laser is used as the source. Computer modeling, high resolution spectroscopy, in-laboratory measurements and outdoor field measurements are all being investigated with the common objective of providing a sound data base for developing a reliable predictive

code which will be adequate to assess laser performance in most of the proposed operational scenarios in which a DF laser might be used.

Computer models such as the AFCRL line tapes[1] have been available for some time but because of variations in the available source data, spectral line shapes and widths, inaccuracies persist. Laboratory measurements, such as White cell[2,3] and spectrophone measurements[4], have been performed for individual absorbers and scatterers in varying concentrations. The measurements for each constituent absorber are added to produce a total extinction coefficient of a model atmosphere. These measurements are then used to update and adjust existing computer codes. Each measurement, however, is a time consuming process which can reasonably be expected to measure only a few of the possible atmospheric models in which a DF laser may be used. The ability to produce extinction coefficients under such controlled conditions is an important asset, however, since high resolution absorption spectra are extremely sensitive to the concentration of the absorber.

Laboratory measurements provide us with a means of checking the extinction coefficient for a given wavelength in a given atmospheric model. High resolution atmospheric absorption spectra, however, change in a dependent fashion such that neighboring absorption bands play a cooperative role in producing absorption at any one laser line. Thus high resolution spectroscopy measurements of the frequency dependence of the absorption spectrum are being performed and these parameters are being used to update predictive models as well.[5]

1.1 MEASUREMENT OBJECTIVES

The objective of this program was to assess the atmospheric extinction experienced by a DF laser used in an actual outdoor field environment and by comparing these measurements with results obtained in laboratory conditions, to verify the accuracy and the validity of the method.

2.0 EXPERIMENTAL INVESTIGATION

2.1 APPROACH

These measurements were performed with a calibrated bistatic system which measured direct transmission loss over a premeasured range. The experimental measurements consisted essentially of monitoring the DF laser output power at the source while simultaneously measuring the atmospherically attenuated power down range. In order to accomplish this, a small portion of the laser's output power was split off using a beam splitter. This reference beam was then calibrated to the output of the laser for each of the wavelengths considered. This arrangement allowed simultaneously the measurement of both the laser output and the received power down range. Each of the respective signals was averaged for at least 1000 pulses of the laser's output.

The total extinction coefficient follows then from Lambert's law:

$$\frac{I}{I_o} = \exp\left(-K_{ext}\, L\right) \qquad (1)$$

where I is the received power down range, I_o is the laser output power at the source, L is the range in km and K(ext) is the total extinction coefficient in km^{-1}. The total extinction coefficient is given by

$K_{ext} = K_m + \sigma_m + K_a + \sigma_a$ where: (2)

K_m = molecular absorption coefficient

σ_m = molecular scattering coefficient

K_a = aerosol absorption coefficient

σ_a = aerosol scattering coefficient

The measurements obtained in this program yield a direct determination of K_{ext} but do not directly yield any of its components. However, if one considers that $\sigma_m \simeq o$ for these wavelengths and that $K_a + \sigma_a$ (the aerosol attenuation coefficient) is known accurately then:

$$K_{ext} = K_m + (K_a + \sigma_a)$$

and

$$K_m = K_{ext} - (K_a + \sigma_a)$$

2.2 EXPERIMENTAL INSTRUMENTATION

A block diagram of the entire experimental configuration is shown in Figure 1. The basic configuration consisted of a laser transmitter and a down range receiver consisting of a large mirror and associated electronics. The single line output from a pulsed DF TEA (Transversely Excited at Atmospheric Pressure) laser is focused through a spectral filter, combined coaxially with a HeNe (Helium Neon) laser, expanded and transmitted 2000 feet down range. The large receiver focuses the beam onto a pyroelectric detector where the signal was analyzed for later comparisons with the signal detected at the transmitter. The experimental apparatus will be described separately in detail, while succeeding parts of Section 3 will discuss the data and conclusions.

2.3.1 TRANSMITTER STATION

The laser shown in Figure 1 is a Lumonics DF TEA laser[6]. The laser operates in the unstable resonator configuration and is equipped with a diffraction grating which allows tuning to a single line. In order to eliminate the superradiant background attendant to this laser configuration, an additional spectral filter was added to improve the spectral purity of the output.

The Lumonics Laser has the following specifications:

Pulse energy on dominant DF lines	30 mj/pulse
Far Field Peak Power	5KW
Optical Pulse Width	500 nsec
Pulse-to-Pulse Amplitude Stability	1% at 1 pps 10-15% at 5 pps

The short pulse nature of the laser output made detector selection difficult. Additionally, the laser was excited by spark gap generated

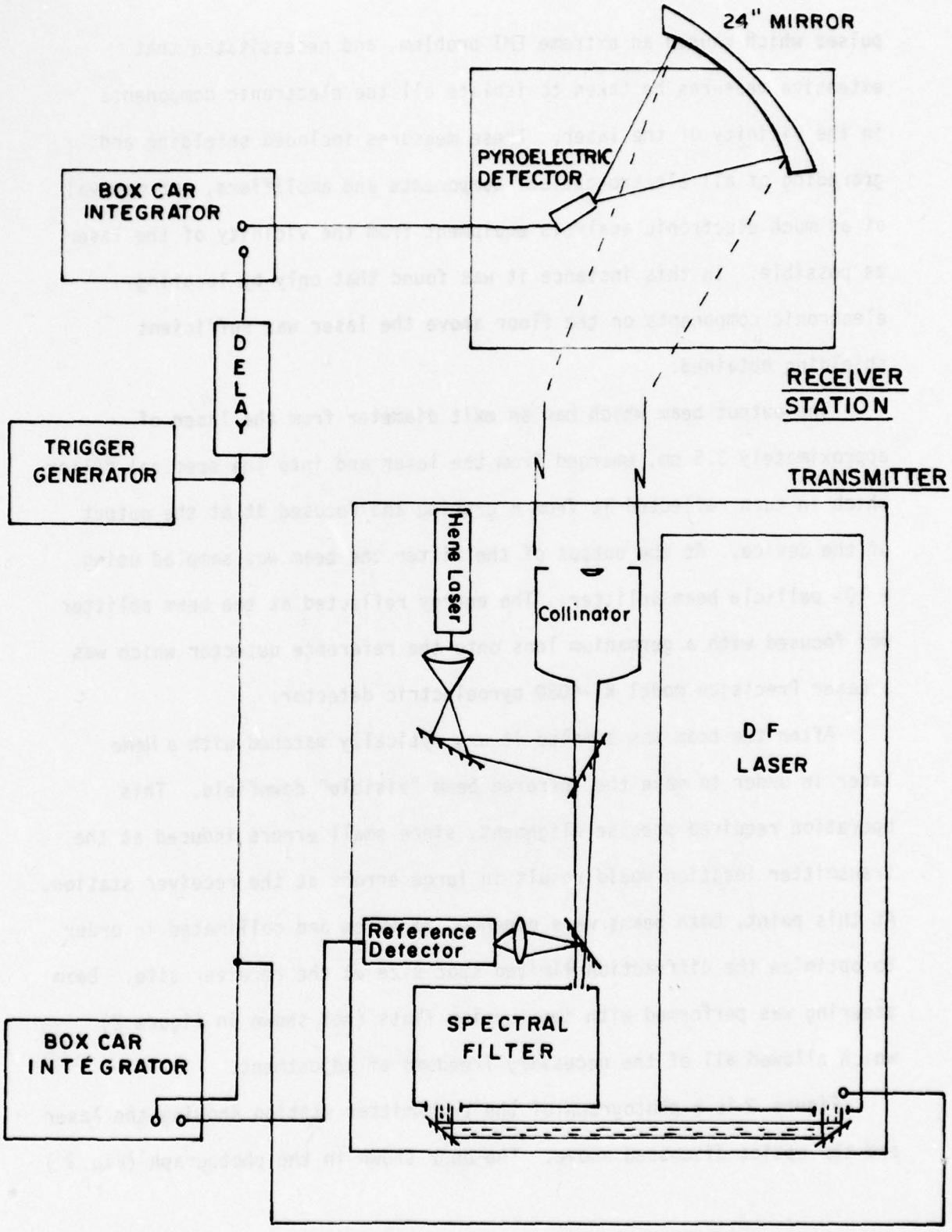

FIGURE 1. EXPERIMENTAL CONFIGURATION

pulses which caused an extreme EMI problem and necessitated that extensive measures be taken to isolate all the electronic components in the vicinity of the laser. These measures included shielding and grounding of all electro-optical components and amplifiers, and removal of as much electronic analysis equipment from the vicinity of the laser as possible. In this instance it was found that only by locating electronic components on the floor above the laser was sufficient shielding obtained.

The output beam which had an exit diameter from the laser of approximately 3.5 cm, emerged from the laser and into the spectral filter which in turn reflected it from a grating and focused it at the output of the device. At the output of the filter the beam was sampled using a 10% pellicle beam splitter. The energy reflected at the beam splitter was focused with a germanium lens onto the reference detector which was a Laser Precision model KT-4080 pyroelectric detector.

After the beam was sampled it was optically matched with a HeNe laser in order to make the infrared beam "visible" downfield. This operation required precise alignment, since small errors induced at the transmitter location would result in large errors at the receiver station. At this point, both beams were expanded to 10 cm and collimated in order to optimize the diffraction limited spot size at the receiver site. Beam steering was performed with two turning flats (not shown in figure 2) which allowed all of the necessary freedoms of adjustment.

Figure 2 is a photograph of the transmitter station showing the laser and the optics discussed above. The door shown in the photograph (Fig. 2)

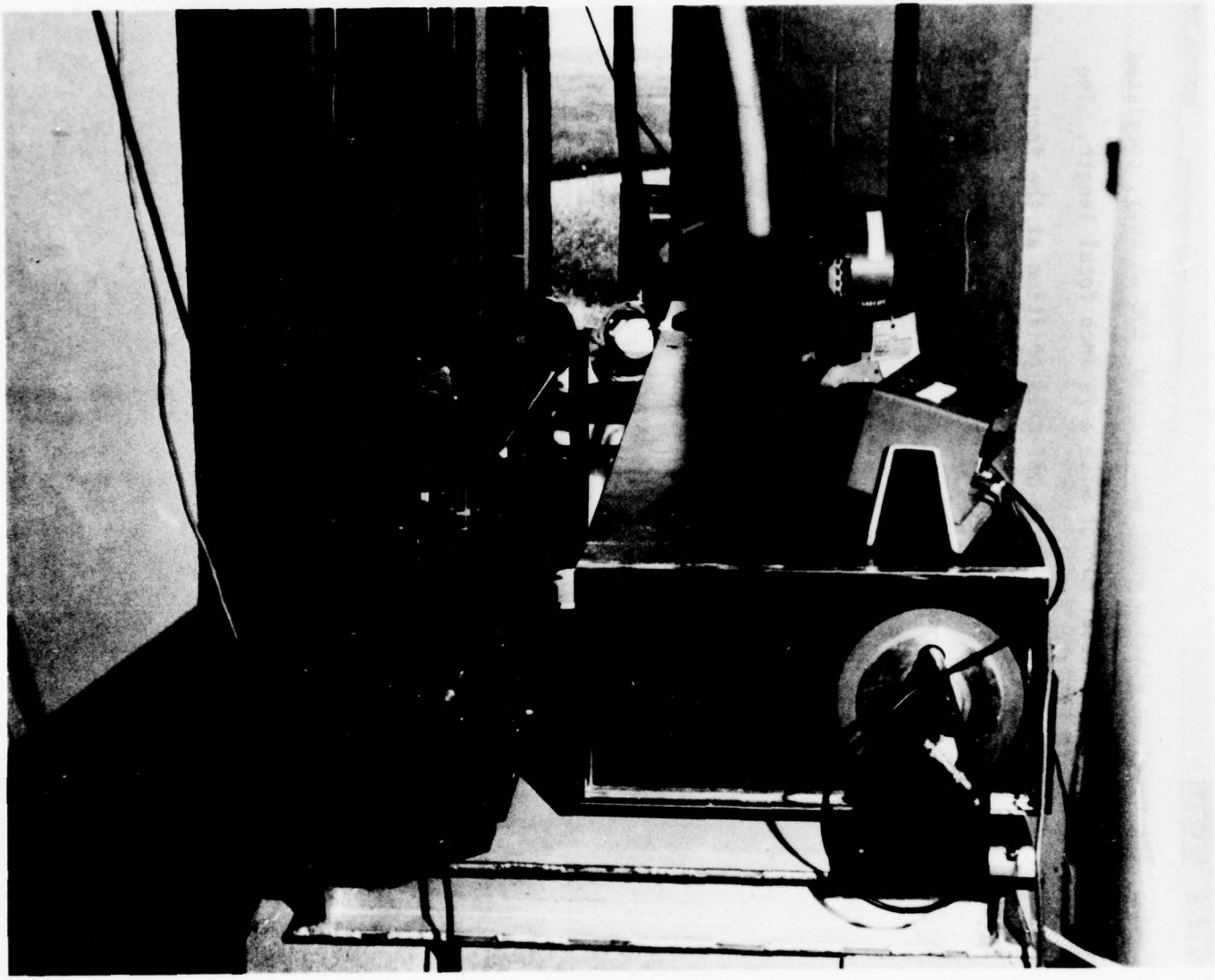

FIGURE 2 TRANSMITTER STATION

served as the output aperture to the test range which is shown in the background.

2.2.2 RECEIVER STATION

The receiver station which was located .606 km away, consisted of a 24 inch polished metal mirror with a 78 inch focal length. The receiver detector was located in an off-axis position at the focus of the mirror. The remaining instrumentation was timing and signal analysis equipment which is discussed below.

2.3 SIGNAL MEASUREMENT

The measurement of transmittance on a single line was time consuming and logistically clumsy because of the distance between the transmitter and receiver and the need for constant recalibration. The signal levels at both the transmitter and receiver were measured using two Laser Precision Model KT-4080 matched pyroelectric detectors both of which were provided with Laser Precision KTH-101 preamplifiers. Prior to making any signal measurements each detector was checked for linearity over the power levels which were expected. Although the optical pulses had an actual pulse width of approximately 500 μsec, the output of the detector systems yielded a pulse several milliseconds wide, the peak of which was linearly proportional to the peak laser pulse power. Thus the signal measuring systems were gated so as to sample the peak outputs of the detector systems. This was accomplished by using two PAR Model 160L Boxcar Integrators which both sampled and integrated successive chains of pulses. Each measurement consisted of the average of 1000 peak power samples.

A single measurement scenario consisted first of bringing the receiver components directly in front of the transmitter where the ratio of the output signal level at this position and the reference signal level was obtained. This ratio provided a calibrated measure of the laser output and did not require a detailed measurement of the spectral transmission and reflection of the various individual optical components in both the transmitter and receiver configurations. However, since the components of the transmitter are spectrally dependent it was necessary to take this ratio for a measurement at each different wavelength. Since the optics

were exposed to harmful and degrading conditions the ratio was taken for each individual measurement to insure that dirt, dust and other deleterious effects did not change the calibration.

After this baseline calibration was established, the receiver components were returned to the receiver station. A signal level measurement at that location was then made and compared to the signal level at the transmitter's reference detector. Thus, if I_o was the transmitter output, I_{ref} was the signal level at the reference detector, I_{rec} was the signal level measured at the receiver and $r(\lambda)$ is the initial calibration ratio, then

$$r(\lambda) = \frac{I_o}{I_{ref}}$$

Since $$I_o = I_{ref}\, r(\lambda)$$

$$\frac{I_{rec}}{I_o} = e^{-K(\lambda)\,(.606)}$$

$$K(\lambda) = \frac{-1}{.606} \ln \frac{I_{rec}}{I_{ref}} \cdot r(\lambda)$$

$K(\lambda)$ then was total extinction coefficient for the particular wavelength under investigation.

In selecting detectors for this experiment the requirements were driven by the need for a detector which was fast enough to respond to the 30 nanosecond rise time of the laser's output pulse and still have the desired responsivities at the power levels expected down range. The

output powers expected from the laser system for the selected wavelengths are listed below:

Spectral Designation	Wavelength (microns)	Expected Output Per Pulse (kw)
2-1P(8)	3.801	36
2-1P(9)	3.838	30
3-2P(8)	3.927	26
2-1P(6)	3.731	28

The expected transmissivity at these wavelengths was calculated using total attenuation coefficients derived from the AFCRL tapes? The transmission at the selected wavelengths is listed below for a Mid-latitude Summer and Winter model for clear (15km visibility) and hazy conditions (5km visibility).

Spectral	Clear		Hazy	
Designation	Winter	Summer	Winter	Summer
2-1P(8)	.98	.98	.91	.90
2-1P(9)	.98	.97	.90	.91
3-2P(8)	.98	.96	.90	.90
2-1P(6)	.97	.95	.91	.80

The relatively high transmission characteristics predicted for these wavelengths clearly indicate that the detectors would not be power limited at the receiver. The detectors chosen were Laser Precision Pyroelectric KT-4080 detectors which had the following characteristics:

Current Responsivity	2μ Amps/Watt
Spectral Response	UV to 74 μm
NEP (10μ, 100Hz, 1) Max	4×10^{-10} Watts
D* (10μ, 100Hz, 1mm^2), Min	2.0×10^{8} cm Hz$^{1/2}$ Watt
Temperature Coefficient	.15%/^{o}C

The advantage of selecting these detectors was that they did not require operation at 77^{o}k as do most sensitive infrared detectors and thus did not require liquid nitrogen cooling. This made operation in the field easier and still maintained the required detector sensitivities.

3.0 RESULTS AND CONCLUSIONS

3.1 TEST ENVIRONMENT

Measurements made in this program were performed on the Advanced Optical Test Range of the Verona Test Annex at Rome Air Development Center.

The specific location of the test site should be considered when attempting to apply an appropriate atmospheric model in comparing the data to predictions. The test range is situated in north central New York state, surrounded by farmland and wooded terrain and is located approximately 15 miles from the nearest urban environment.

A photograph of the range is shown in Figure 3. The DF laser beam originated from the first floor of the test facility and was received in a small shed which housed the receiver instrumentation down range. In this way, the laser beam radiated across flat terrain which consisted of low lying wet grassland and wet swampy regions.

The propagation path varied from 3 to 15 feet above the ground surface. Measurements were made in a variety of meteorological conditions but predominantly in the late winter and spring.

Since adequate instrumentation was not available to precisely characterize the local test environment a few qualitative observations are in order to aid in analyzing the results. The transmission path in this program hugged relatively close to ground level passing over both dry and very wet regions of the range. These considerations would tend to indicate that the local atmosphere through which the beam passed

FIGURE 3 ADVANCED OPTICAL TEST RANGE

contained higher and graduated levels of water vapor than were measured at the receiver and transmitter locations. Additionally, the proximity to the wet terrain would indicate that there were high levels of hydrosol concentration, especially when the dew point and ambient temperature were close. This is thought to be the primary cause of the discrepancies between the measured results and the predictions. The other qualitative observation which bears on the results would be the presence of decaying vegetation along the propagation path which may indicate the possibility of high concentrations of methane.

The distance of the range from urban centers and the relatively small size of those centers would indicate that the concentrations of urban or industrial pollutants were relatively low and not a major variable in the measurements program.

3.2 RESULTS

Measurements were completed for the following lines: 2-1P(8), 2-1P(6), 3-2P(8) and 2-1P(9). The results and measurement conditions are tabulated in Table 1 Temperature conditions are given in both ^{o}K and ^{o}F for convenience and represent the average of a measurement taken at the receiver and transmitter section before and after each measurement. The partial water vapor pressure was derived from dew point depression measurements made at the transmitter site after each measurement. Visibility data was taken using a conventional airport transmissiometer located some 15 miles away. This measurement is purely an indication of the general visibility conditions (and aerosol content) of the region and is not purported to be an accurate indication of the true aerosol content of the actual transmission

Line Designation	Wavelength (Microns)	Transmission (%)	T (°F)	T (°K)	H_2O Pressure (TORR)	Visibility (mi)	Absorp Coef (km^{-1})
2-1P(8)	3.801	56	80.4°	300°	11.23	3	9.5E-1
		62.1	86.1°	303.1°	10.14	10	7.82E-1
		66.0	86.04	303.1	15.76	3	6.83E-1
		69.0	76.7	298.0	14.9	15	6.09E-1
		92.0	61.9	289.7	4.05	10	1.37E-1
		94.2	61.9	289.7	4.05	10	9.81E-2
		94.6	61.9	289.7	4.05	10	9.11E-2
		95.56	61.9	289.7	4.05	10	7.45E-2
		95.57	61.9	289.7	4.05	10	7.44E-2
		93.61	68.7	293.5	3.15	10	1.08E-1
		98.60	68.7	293.5	3.15	10	2.3E-2
		98.03	68.7	293.5	3.15	10	3.0E-2
		93.16	68.7	293.5	3.15	10	1.2E-1
2-1P(9)	3.838	63.83	76.9	298.1	12.66	10	7.37E-1
		67.74	76.9	298.1	12.66	10	6.40E-1
		68.31	76.9	298.1	12.66	10	6.25E-1
		64.85	76.9	298.1	12.66	10	7.11E-1
3-2P(8)	3.927	2.65	71.8	295.2	9.45		5.96
		2.1	71.8	295.2			6.4
2-1P(6)	3.731	59.5	70.9	294.7	9.8	10	8.52E-1
		60.9	73.0	295.9	8.76	10	8.14E-1

TABLE 1 - TABULATION OF RESULTS

path.

Table 2 is a tabulation of the latest laboratory measurements made by various researchers through out the country compiled through the courtesy of Dr. R.K. Long of Ohio State University. The table indicates the fractional molecular absorption (not total extinction) expected for concentrations of the major absorbers at DF wavelengths. The absorber concentrations are based on the Mid-latitude Summer model and on the water vapor concentrations measured during the tests. The resulting total molecular absorption coefficient is shown in the last column of this table and has been obtained by adding the contributions of each of the constituent gases indicated (N_2O, CH_4, CO_2, N_2, H_2O). This value indicates the total molecular absorption measured under laboratory conditions and does not compensate for the effects of aerosols and hydrosols in the path.

The table shown in Table 3 demonstrates a comparison between some of the outdoor measurements and the corresponding laboratory measurements. For some of the wavelengths there is no existing laboratory data for comparison. The laboratory measurement and field measurement for a given line are shown in columns five and six respectively. The percentage difference between these two measurements is shown in column seven. Note that the outdoor measurement includes the effects of aerosol attenuation while the laboratory measurement is only a measure of molecular absorption Thus, the percentage difference between the two values is a measure of the sum of both the aerosol contributions to extinction and the experimental error. In the case of the 2-1P(8) line, for which most of the comparative

Line ID	λ (Microns)	T (°K)	H_2O Press (Torr)	(a) N_2O (Km^{-1})	(b) CH_4 (Km^{-1})	(c) CO_2 (Km^{-1})	(d) N_2 (Km^{-1})	(e) H_2O (Km^{-1})	TOTAL (Km^{-1})
2-1 P(8)	3.801	300	11.23	0	8.6E-4	5.3E-4	1.9E-3	3E-2	3.33E-2
		303.1	10.14	0	8.6E-4	5.3E-4	1.9E-3	2.7E-2	3.03E-2
		303.1	15.75	0	8.6E-4	5.3E-4	1.9E-3	4.2E-2	4.53E-2
		298	14.95	0	8.6E-4	5.3E-4	1.9E-3	3.98E-2	4.31E-2
2-1 P(6)	3.731	294.7	9.83	0	1.52E-3	1.9E-5	0	5.1E-2	5.25E-2
		295.9	8.76	0	1.52E-3	1.9E-5	0	4.6E-2	4.75E-2
3-2 P(8)	3.927	295.2	9.45	2.14E-2	4.11E-2	4.21E-4	1.86E-2	2.05E-2	4.0E-2
2-1 P(8)	3.801	289.7	4.05	0	8.59E-4	5.3E-4	1.9E-3	1.08E-2	1.41E-2

(a) Long, OSU[7]

(b) 3-2P(8) Deaton[9]; 2-1P(6) and 2-1P(8) OSU[8]

(c) 2-1P(8) OSU[8]; 2-1P(6) and 3-2P(8) Myers[10]

(d) Burch, et. al[11]

(e) Long, OSU[8]

TABLE 2 - Table of Absorption Coefficients compiled from Laboratory Measurements

Line Design.	H_2O Pressure	Dew Point Depress.	Humidity	Lab Meas Absorp Coef	Field Meas Absorp Coef	% Diff.	Aerosol Ext Coefficient	Adjusted. Coef	% Diff.
	(TORR)	(^oF)	(%)	(Km^{-1})	(Km^{-1})	(%)	(Km^{-1})	(Km^{-1})	(%)
2-1P(8)	11.23	11	64	3.33E-2	9.5E-1	96	.13E-1	1.6E-1	83.1
	10.14	34	52	3.03E-2	7.82E-1	96	.69E-2	9.9E-2	87.3
	15.76	21	52	4.53E-2	6.83E-1	93	1.3E-1	1.8E-1	73.6
	14.9	13.2	62	4.31E-2	6.09E-1	92	4.7E-2	9.0E-2	85.2
	4.05	32	37	1.41E-2	1.37E-1	89	6.9E-2	8.3E-2	39.4
	4.05	32	37	1.41E-2	9.81E-2	85	6.9E-2	8.3E-2	15.4
	4.05	32	37	1.41E-2	9.11E-2	81	6.9E-2	8.3E-2	8.8
	4.05	32	37	1.41E-2	7.45E-2	84	6.9E-2	8.3E-2	11.4
	4.05	32	37	1.41E-2	7.44E-2	81	6.9E-2	8.3E-2	11.4
	3.15	41	29	1.17E-2	1.08E-1	89	6.9E-2	8.07E-2	25.3
	3.15	41	29	1.17E-2	2.3E-2	49	6.9E-2	8.07E-2	
	3.15	41	29	1.17E-2	3.0E-2	61	6.9E-2	8.07E-2	
	3.15	41	29	1.17E-2	1.2E-1	90	6.9E-2	8.07E-2	
3-2P(8)	9.45	20		4.0E-2	5.90				
	9.45	20		4.0E-2	6.4				
2-1P(6)	9.83	14		5.25E-2	8.52E-1				
	8.76	14		4.75E-2	8.14E-1				

TABLE 3 - COMPARISON OF RESULTS

data exists, the percentage differences range from 49% to 96%.

In order to estimate the possible effects of aerosol extinction on the measurement an aerosol extinction coefficient was derived by interpolating existing aerosol data[7] for the visibilities shown in column seven of Table 1. This coefficient was then added to the laboratory measurements and the results are shown in column nine. Thus, the last column in Table 3 represents the percentage difference between the field measurements and the sum of the laboratory measurement and the computed aerosol extinction coefficients. The differences for this comparison range 8.8% to 87.3%. Although the magnitudes of the discrepancies have been decreased they are still reasonably large.

3.3 CONCLUSIONS

In examining the results and residual differences between the adjusted laboratory measurements one must conclude that either the estimation of the effects aerosols have on transmission is too small or anomalies in the propagation path itself have given rise to the differences. Since the beam path did hug relatively close to ground level and passed over alternating wet and dry regions, it is entirely possible that the local atmosphere through which the beam passed contained higher or lower water vapor graduations than either of the two end points. The consequent inhomogeneity in the path would very well contribute to some of the discrepancies.

Additionally, the data from which the aerosol coefficient was derived did not contain any compensation for the effects of water vapor content upon the aerosol size distribution or the possible presence of hydrosols. If one examines Figures 4 and 5 the presence of this effect seems evident. As either the dew point depression approaches zero or the relative humidity rises the percentage differences in the measurements converge to higher values.

These two effects would lead one to question the value of measurements made at ground level over inhomogeneous terrain or measurements made where adequate compensation for the interplay of water vapor content and aerosol size distribution cannot be made.

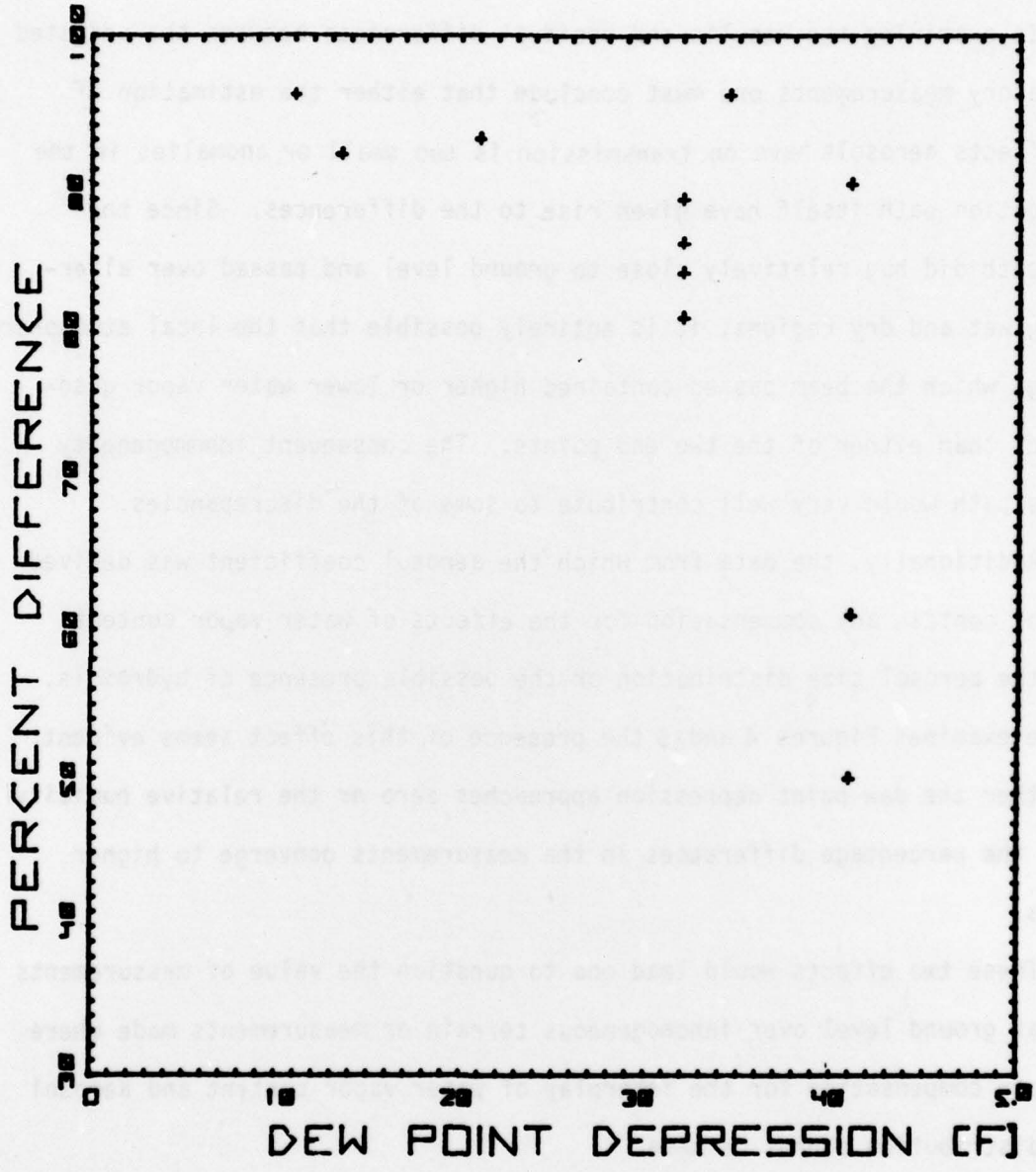

FIGURE 4 - DEW POINT DEPRESSION VS PERCENT DIFFERENCE OF LABORATORY AND FIELD MEASUREMENTS

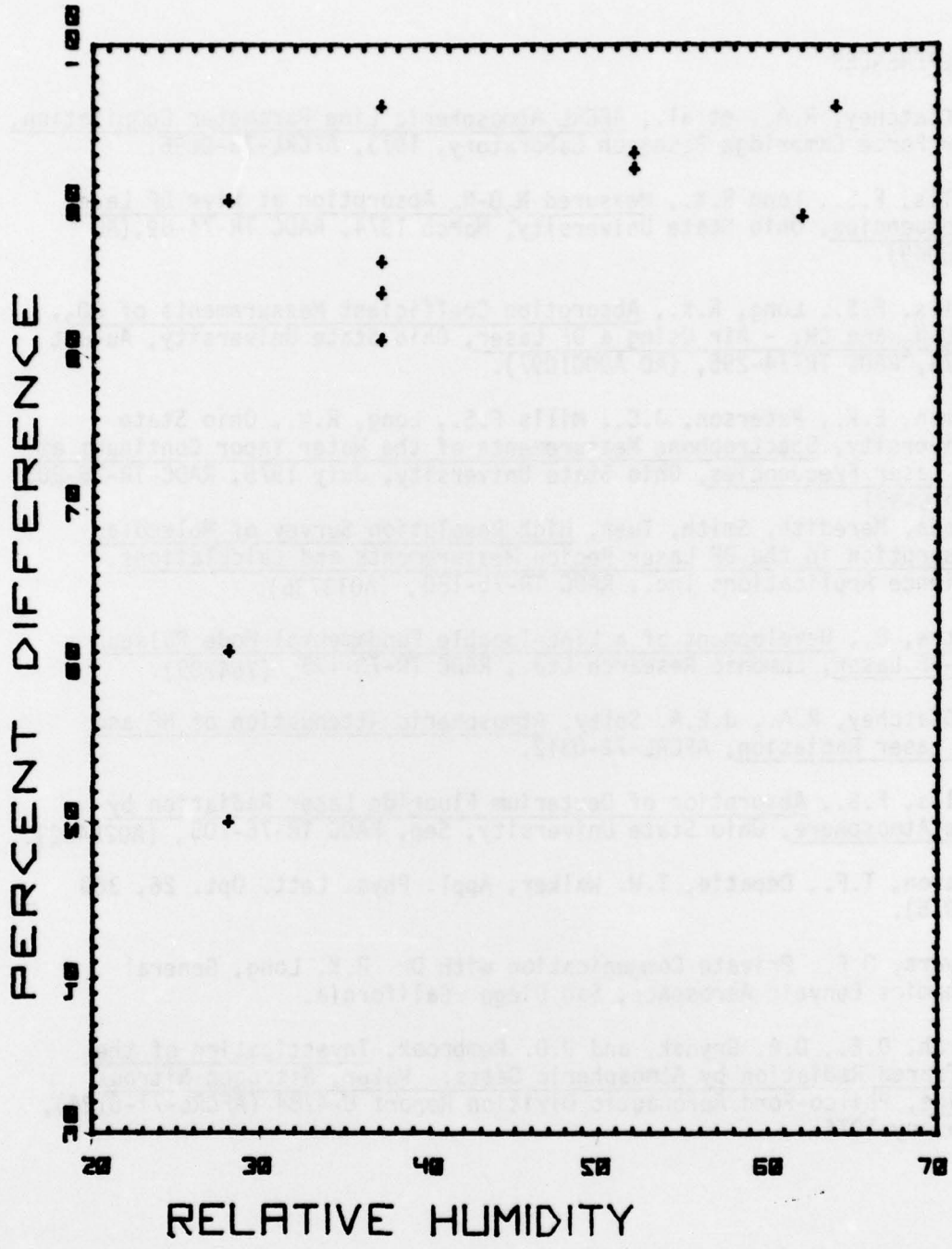

FIGURE 5 - RELATIVE HUMIDITY VS PERCENT DIFFERENCE OF LABORATORY AND FIELD MEASUREMENTS

4.0 REFERENCES

1. McClatchey, R.A., et.al., AFCRL Atmospheric Line Parameter Compilation, Air Force Cambridge Research Laboratory, 1973, AFCRL-73-0096.

2. Mills, F.S., Long R.K., Measured N_2O-N_2 Absorption at Five DF Laser Frequencies, Ohio State University, March 1974, RADC TR-74-89,(AD 778949).

3. Mills, F.S., Long, R.K., Absorption Coefficient Measurements of CO_2, HDO-N_2 and CH_4 - Air Using a DF Laser, Ohio State University, August 1974, RADC TR-74-295, (AD A0001097).

4. Damon, E.K., Peterson, J.C., Mills F.S., Long, R.K., Ohio State University, Spectrophone Measurements of the Water Vapor Continuum at DF Laser Frequencies, Ohio State University, July 1975, RADC-TR-75-203, (A016435).

5. Woods, Meredith, Smith, Tuer, High Resolution Survey of Molecular Absorption in the DF Laser Region Measurements and Calculations, Science Applications Inc., RADC TR-75-180, (A013736).

6. Rothe, D., Development of a Line-Tunable Fundamental-Mode Pulsed HF-DF Laser, Lumonic Research Ltd., RADC TR-73-173, (764709).

7. McClatchey, R.A., J.E.A. Selby, Atmospheric Attenuation of HF and DF Laser Radiation, AFCRL-72-0312.

8. Mills, F.S., Absorption of Deuterium Fluoride Laser Radiation by the Atmosphere, Ohio State University, Sep, RADC TR-76-105, (A025402).

9. Deaton, T.F., Depatie, T.W. Walker, Appl. Phys. Lett. Opt. 26, 300 (1975).

10. Meyers, O.E., Private Communication with Dr. R.K. Long, General Dynamics Convair Aerospace, San Diego, California.

11. Burch, D.E., D.A. Grynak, and J.D. Pembrook, Investigation of the Infrared Radiation by Atmospheric Gases: Water, Nitrogen Nitrous Oxide, Philco-Ford Aeronautic Division Report U-4784 (AFCRL-71-0124), January 1974.

METRIC SYSTEM

BASE UNITS:

Quantity	Unit	SI Symbol	Formula
length	metre	m	...
mass	kilogram	kg	...
time	second	s	...
electric current	ampere	A	...
thermodynamic temperature	kelvin	K	...
amount of substance	mole	mol	...
luminous intensity	candela	cd	...

SUPPLEMENTARY UNITS:

plane angle	radian	rad	...
solid angle	steradian	sr	...

DERIVED UNITS:

Acceleration	metre per second squared	...	m/s
activity (of a radioactive source)	disintegration per second	...	(disintegration)/s
angular acceleration	radian per second squared	...	rad/s
angular velocity	radian per second	...	rad/s
area	square metre	...	m
density	kilogram per cubic metre	...	kg/m
electric capacitance	farad	F	A·s/V
electrical conductance	siemens	S	A/V
electric field strength	volt per metre	...	V/m
electric inductance	henry	H	V·s/A
electric potential difference	volt	V	W/A
electric resistance	ohm		V/A
electromotive force	volt	V	W/A
energy	joule	J	N·m
entropy	joule per kelvin	...	J/K
force	newton	N	kg·m/s
frequency	hertz	Hz	(cycle)/s
illuminance	lux	lx	lm/m
luminance	candela per square metre	...	cd/m
luminous flux	lumen	lm	cd·sr
magnetic field strength	ampere per metre	...	A/m
magnetic flux	weber	Wb	V·s
magnetic flux density	tesla	T	Wb/m
magnetomotive force	ampere	A	...
power	watt	W	J/s
pressure	pascal	Pa	N/m
quantity of electricity	coulomb	C	A·s
quantity of heat	joule	J	N·m
radiant intensity	watt per steradian	...	W/sr
specific heat	joule per kilogram-kelvin	...	J/kg·K
stress	pascal	Pa	N/m
thermal conductivity	watt per metre-kelvin	...	W/m·K
velocity	metre per second	...	m/s
viscosity, dynamic	pascal-second	...	Pa·s
viscosity, kinematic	square metre per second	...	m/s
voltage	volt	V	W/A
volume	cubic metre	...	m
wavenumber	reciprocal metre	...	(wave)/m
work	joule	J	N·m

SI PREFIXES:

Multiplication Factors	Prefix	SI Symbol
1 000 000 000 000 = 10^{12}	tera	T
1 000 000 000 = 10^{9}	giga	G
1 000 000 = 10^{6}	mega	M
1 000 = 10^{3}	kilo	k
100 = 10^{2}	hecto*	h
10 = 10^{1}	deka*	da
0.1 = 10^{-1}	deci*	d
0.01 = 10^{-2}	centi*	c
0.001 = 10^{-3}	milli	m
0.000 001 = 10^{-6}	micro	μ
0.000 000 001 = 10^{-9}	nano	n
0.000 000 000 001 = 10^{-12}	pico	p
0.000 000 000 000 001 = 10^{-15}	femto	f
0.000 000 000 000 000 001 = 10^{-18}	atto	a

* To be avoided where possible.

MISSION
of
Rome Air Development Center

RADC plans and conducts research, exploratory and advanced development programs in command, control, and communications (C^3) activities, and in the C^3 areas of information sciences and intelligence. The principal technical mission areas are communications, electromagnetic guidance and control, surveillance of ground and aerospace objects, intelligence data collection and handling, information system technology, ionospheric propagation, solid state sciences, microwave physics and electronic reliability, maintainability and compatibility.